Journal of Fluorescence (2018) 28:1421–1430
https://doi.org/10.1007/s10895-018-2317-1

ORIGINAL ARTICLE

Spectroscopic Study of Solvent Polarity on the Optical and Photo-Physical Properties of Novel 9,10-bis(coumarinyl)anthracene

Hasnaa M. Fahmy[1] · Hamed M. Kandel[1] · Hamdan A. S. Al-shamiri[2,3] · Nabel A. Negm[4] · Ahmed H. M. Elwahy[5] · Maram T. H. Abou Kana[1]

Received: 10 September 2018 / Accepted: 14 October 2018 / Published online: 21 October 2018

Abstract

Novel 7,7′-((anthracene-9,10-diylbis(methylene))bis(oxy))bis(4-methyl-2*H*-chromen-2-one) (BisCA) was prepared as fluorescent probe. The chemical structure of the novel BisCA was confirmed by spectroscopic data as well as elemental analyses. The solvatochromic characteristics of the new proble and its precursors were investigated in different solvents including, ethanol, DMF and toluene as protic polar, aprotic polar and non-polar solvents, respectively. Photo-physical parameters of probes, such as fluorescence quantum yields, fluorescence lifetime of excited state, radiative and non-radiative decay, were assessed in different media. The intermolecular H-bond effect on absorption and excitation spectra of the novel probe was reported in different solvents. Also, Onsager cavity radius and dipole moment of ground state and excited state of the probe were calculated as described by Bakhshiev and Reichardt methods.

Keywords Optical property · Solvent polarity · H-bond · Spectroscopy · Novel dye · Solvatochromic characteristic

Introduction

Fluorescent dyes attract attention in the last decades owing to their different optical microscopic applications such as OLEDs [1], anti-forgery markers. [2], diverse materials as sunscreens [3], dye-injection solar cells [4], phosphorescent lighting strips [5], selective probes [6–8], bio-labels, [9], fluorescent markers, [10] and solid-state pH indicators [11].

The solvents have different effects on geometrical structure of solute molecules and their spectroscopic behavior have been previously monitored [12–23]. In this respect, the Stokes shift, which is the difference (in wavelength or frequency units) between positions of the band maxima of the absorption and emission spectra of the same electronic transition, have also studied as a function of; 1) the dielectric effects, which is, from a molecular point of view, the dipolar interaction between the solute and the solvent molecules; 2) the dispersive interaction because of van der Waals forces which exist in solvent-solute system; 3) the specific interaction between the solvent and the solute molecules, e.g., hydrogen bonding, electron transfer,.. etc.; 4) the aggregation effect between solute molecules; this effect changes with changing solute concentrations and may be neglected at low solute concentration; 5) the electrochemical effects, which is the changes in the degree of dissociation of a solute in different solvents; this effect is studied by varying the pH of the medium; 6) the intermolecular resonance effects which is important in emission spectra study.

On the other hand, upon photo-excitation [18, 24–26], intermolecular hydrogen bonding significantly strengthened in the electronic excited state resulting in an important role in photochemistry, such as intermolecular charge transfer [18], fluorescence quenching [24], excited-state proton transfer [25] and tuning effects on photochemistry [26].

In continuation of our recent interest in designing and preparing new dyes [27–29], we report herein on the synthesis of

✉ Maram T. H. Abou Kana
mabou202@niles.edu.eg

[1] National Institute of Laser Enhanced Sciences, Cairo University, Giza, Egypt

[2] Physics Department, Faculty of Applied Science, Taiz University, Taiz, Yemen

[3] Physics Department, Faculty of Science, University of Bisha, Bisha, Kingdom of Saudi Arabia

[4] Petrochemicals Department, Egyptian Petroleum Research Institute, Nasr City, Cairo, Egypt

[5] Chemistry Department, Faculty of Science, Cairo University, Giza, Egypt

new fluorescent probe and studying the effect of different solvents on its optical and photophysical properties.

Experimental

General

Melting points were determined in open glass capillaries with a Gallenkamp apparatus and were not corrected. The infrared spectra were recorded in potassium bromide disks on a PyeUnicam SP3–300 and Shimadzu FTIR 8101 PC infrared spectrophotometer. The ^{1}H and ^{13}C NMR spectra were determined on a Varian Mercury VX 300 NMR spectrometer using TMS as an internal standard and DMSO-d6 as a solvent. Mass spectra were measured on a GCMS-QP1000 EX spectrometer at 70 eV. Elemental analyses were carried out at the Microanalytical Center of Cairo University, Giza, Egypt. 7-Hydroxy-4-methylcoumarin **(1)** and 9,10-bis(bromomethyl)anthracene (**2**) were purchased from Sigma-Aldrich.

Synthesis of Novel 9,10-bis(coumarinyl) Anthracene Derivative

Synthesis of the K-Salt of (1)

A solution of each of compounds **1** (10 mmol) and KOH (1.14 g, 20 mmol) in ethanol (10 ml) was stirred at room temperature for 10 min. The solvent was removed in vacuo and the remaining solvent was triturated with dry ether, collected and dried. It was then used in the next steps without further purification.

Synthesis of 7,7′-((anthracene-9,10-diylbis(methylene)) bis-(oxy))bis(4-methyl-2*H*-chromen-2-one) (BisCA) (3)

A solution of each of the potassium salt of **1** (20 mmol) and 9,10-bis(bromomethyl)anthracene (**2**) (10 mmol) in DMF (20 ml) was heated under reflux for 5 min during which time KBr was precipitated. The solvent was then removed in vacuo and the remaining material was washed with water (50 ml) and crystallized from DMF to give compound **3** as orange crystals.; yield: 81%; mp 242 °C; IR: υ max 1714 (C=O) cm^{-1}, ^{1}H NMR (DMSO) δ 2.39 (s, 6H, CH_3), 5.41 (s, 4H, OCH_2), 6.20–7.92 (m, 10H, ArHs, Coumarin H) ppm. MS: m/z 554 (M^+); Anal. for $C_{36}H_{26}O_6$ (554.17), Calcd: C, 77.97; H, 4.73. Found: C, 77.70; H, 5.10.

Specroscopic Analysis

(1 × 10–5 M) Solutions of the new probe 910-bis(coumarinyl) anthracene **3** and its precursors coumarin **1** and anthracene **2** were prepared by mixing 100 μL 1×10^{-3} M in DMF with other solvents to get concentration of 1×10^{-5} M of probes. All solution samples were contained in 1 cm optical-path quartz cells. Absorption and emission spectra were measured using Camspec M501 uv-vis spectrophotometer and PF-6300 spectrofluorometer, respectively.

Polarity Parameters of Solvents and Onsager Cavity Radius Calclations

Solvent polarities play a significant effect on ground and excited sates of fluorescent molecules. Different direct methods for the assessment of the excited state dipole moment such as fluorescence polarization, stark splitting of rotational levels and electric dichroism are known and accurate, but the most common method still based on the solvatochromism analysis of the absorption and fluorescence frequency maxima using either microscopic bulk polarity (E_T^N) or functionized polarities f (n,ε) [30, 31]. In the latter method suggested by Bakhshiev, the Stokes shift between the absorption and fluorescence frequencies maxima is pointed to the dipole moment change on excitation as presented in the following equations [30, 31].

$$\upsilon_a - \upsilon_f = m_1 f(\varepsilon, n) + const. \quad (1)$$

$$\upsilon_a + \upsilon_f = -m_2[f(\varepsilon, n) + 2g(n)] + const. \quad (2)$$

Where; $\upsilon_a$and υ_f are the peak absorption and fluorescence frequencies.

Scheme 1 Synthesis of compound 3 (BisCA)

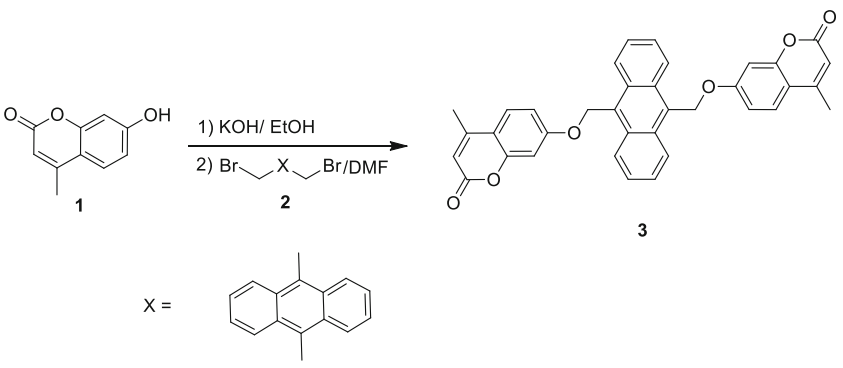

Fig. 1 ^{1}H NMR of BisCA

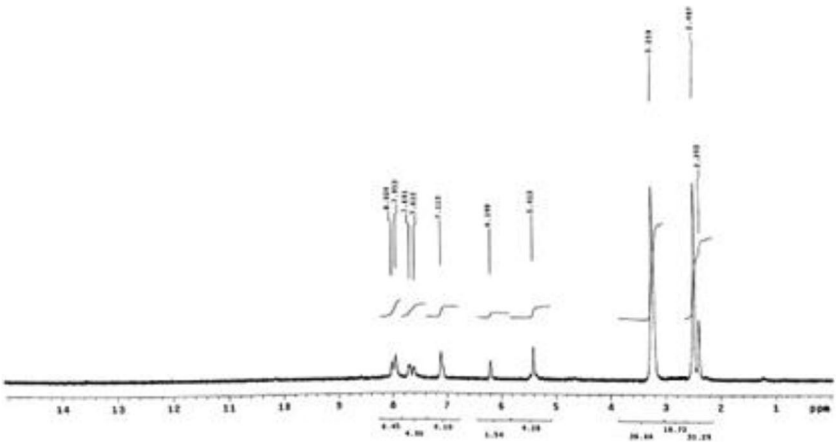

However;

$$f(\varepsilon,n)=\frac{2n^2+1}{n^2+2}\left[\frac{\varepsilon-1}{\varepsilon+2}-\frac{n^2+1}{n^2+2}\right] \tag{3}$$

and

$$g(n)=\frac{3}{2}\left[\frac{n^4-1}{(n^2+2)^2}\right] \tag{4}$$

are the solvent polarity parameters as functions in dielectric permittivity (ε) and refractive index (n) according to Bakhshiev method which express the contributions of the orientation and dispersive-induction-polarization interactions, respectively.

Where;

$$m_1=\frac{2\left(\mu_e-\mu_g\right)^2}{hca^3} \tag{5}$$

is the slope of Eq. (1). And

$$m_2=\frac{2\left(\mu_e+\mu_g\right)^2}{hca^3} \tag{6}$$

is the slope of Eq. (2). Where h is Plank's constant and c, the velocity of light in vacuum whereas μ_g and μ_e are the ground and excited state dipole moments, respectively.

Also, the dipole moment of ground state (μ_g) and excited state (μ_e) parameters can be determined from Eqs. (7) and (8) assuming that the symmetry of the probe molecule remains unchanged through electronic transition, and the ground and excited state dipole moments are parallel [32],

$$\mu_g=\frac{|m_2-m_1|}{2}\left[\frac{hca^3}{2m_1}\right]^{\frac{1}{2}} \tag{7}$$

$$\mu_e=\frac{|m_2+m_1|}{2}\left[\frac{hca^3}{2m_1}\right]^{\frac{1}{2}} \tag{8}$$

Since parameters m_1 and m_2 are linear functions of the solvent polarity parameters f(ε, n) and f(ε, n) + 2 g(n) and can be

Fig. 2 Absorption spectra of 1 × 10^{-5} M three dyes in DMF

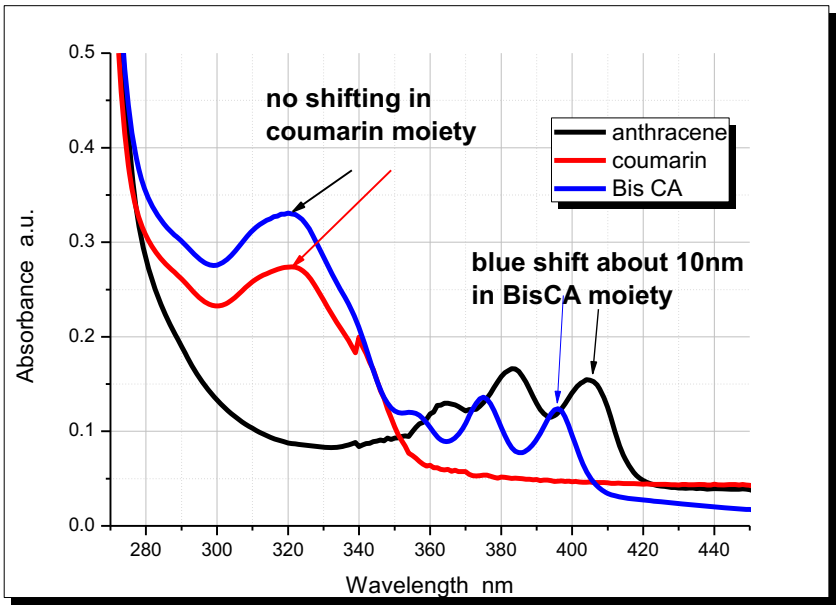

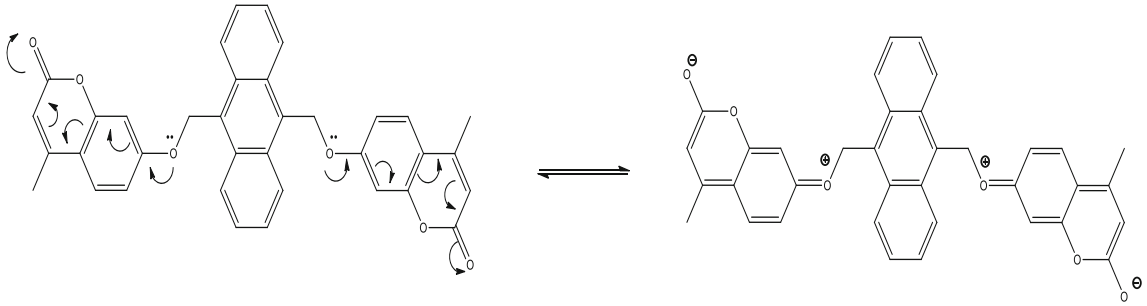

Scheme 2 Intramolecular charge transfer (ICT) in coumarin part of compound 3 (BisCA)

determined from the slopes of straight lines, the Onsager cavity radius (α) can also easily be assessed according to the theory [33–35] that assumed the molecule to be sphere in shape and its Onsager radius can be evaluated using the relation:

$$\alpha = \left({}^{3M}/_{4\pi\delta N}\right)^{1}/_{3} \tag{9}$$

M: is the molecular mass of molecule, δ is the density and N is the Avogadro's number.

On the other hand, Reichardt [36] reported an empirical polarity scale which gave better results of solvatochromic shift of dipolar molecules that depends mainly on microscopic solvent polarity E_T^N rather than on traditionally bulk solvent polarity functions. Accordingly, the excited state dipole moment is determined using Eq. (10) [37].

$$\nu_a - \nu_b = 11307.6\left[\left(\frac{\Delta\mu}{\Delta\mu_B}\right)^2\left(\frac{a_B}{a}\right)^3\right]E_T^N + const. \tag{10}$$

where $\Delta\mu_B$= 9D and a_B= 6.2 Å represents the change in dipole moment on excitation and Onsager radius, respectively, for betaine dye as reference probe, while (Δμ) and (α) are the corresponding quantities for the target probe.

Photo-Physical Properties

Studying of photo-physical properties such as fluorescence quantum yields φ_f (that was obtained by applying a comparative method [38]), fluorescence lifetime, radiative decay and non-radiative decay in different environmental solvent have been the subject of various investigations because of the wealth of information on photochemistry of target probe for various applications.

For determination of fluorescence quantum yield (ϕ_f) using Rhodamine 6G (R6G) in MeOH solution of a quantum yield (ϕ_f) of 0.96 [39] as a reference, the emission spectra were monitored at different wavelengths having the same absorbance intensities of R6G and target probe. To determine the quantum yield of a compound relative to a standard material, a very dilution of dye was used to avoid self-reabsorption phenomena, the following relationship (11) was applied: [40].

$$\phi_u = \phi_s \times \frac{I_u}{I_s} \times \frac{A_s}{A_u} \times \frac{n_u^2}{n_s^2}. \tag{11}$$

Where ϕ_u, I_u and A_u are the fluorescence quantum yields, the areas under emission curve and the absorbance, respectively, of

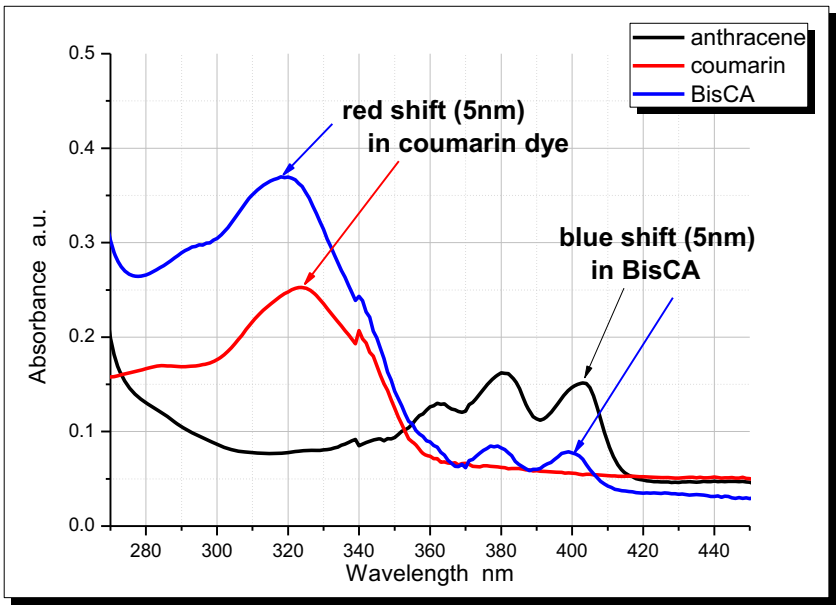

Fig. 3 Absorption spectra of 1 × 10^{-5} M three dyes in ethanol

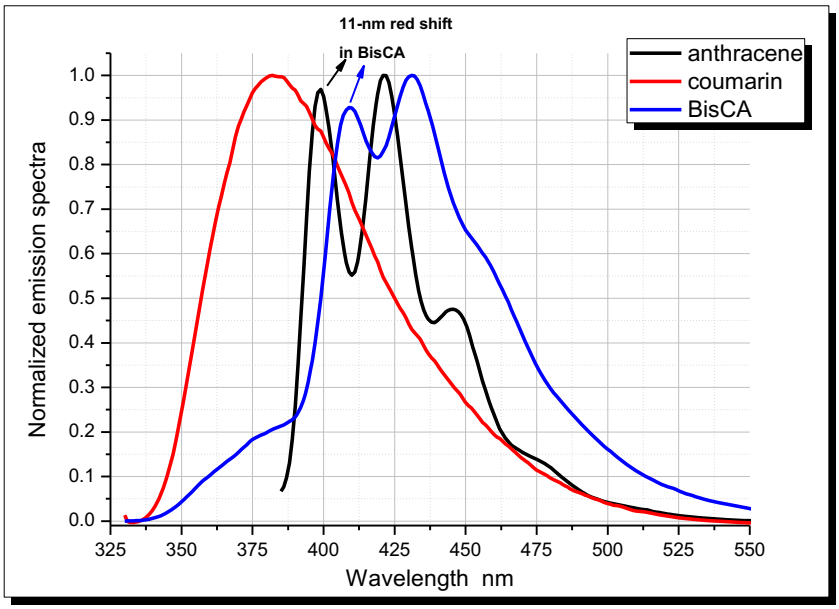

Fig. 4 Normalized emission spectra of 1×10^{-5} M three dyes in DMF

the unknown probe. While, ϕ_s, I_s, $A_s$are those of the standard dye. n_s and n_u are the refractive indices of solvents used.

Other important sequent photo-physical property is the lifetime of excited state which provides significant information about intermolecular kinetics interaction including dimmer formation [41] and different types of energy transfer. Lifetime fluorescence value (τ) is a function of the quantum yield, emission and absorption spectra by means of Eq. (12) [42] as follows:

$$\frac{1}{\tau} = 2.88 \times 10^{-9} n^2 \phi_f^{-1} \frac{\int F(v)dv}{\int v^{-3} F(v)dv} \int \frac{\varepsilon(v)}{v} dv \qquad (12)$$

ν: wavenumber (cm^{-1}), F(ν): intensity of the emitted fluorescence, n: refractive index. Derived from the emission and absorption spectra and the wavelengths (λ) which were converted into wavenumbers (cm^{-1}), the integral values were assessed and consequently the calculated lifetime of fluorescence (τ) was determined.

Oscillator strength Values are calculated by Eq. (13) [43]:

$$f = 4.32 \times 10^{-9} \int \varepsilon(v)dv \qquad (13)$$

Also, the transition dipole moment (μ_{12}) from ground to excited state was calculated in different media by the Eq. (14); where f is related to the transition moment and the Einstein coefficient by the following expressions:

$$\mu_{12}^2 = 2.36 \times 10^{-51} \times f \times \lambda \qquad (14)$$

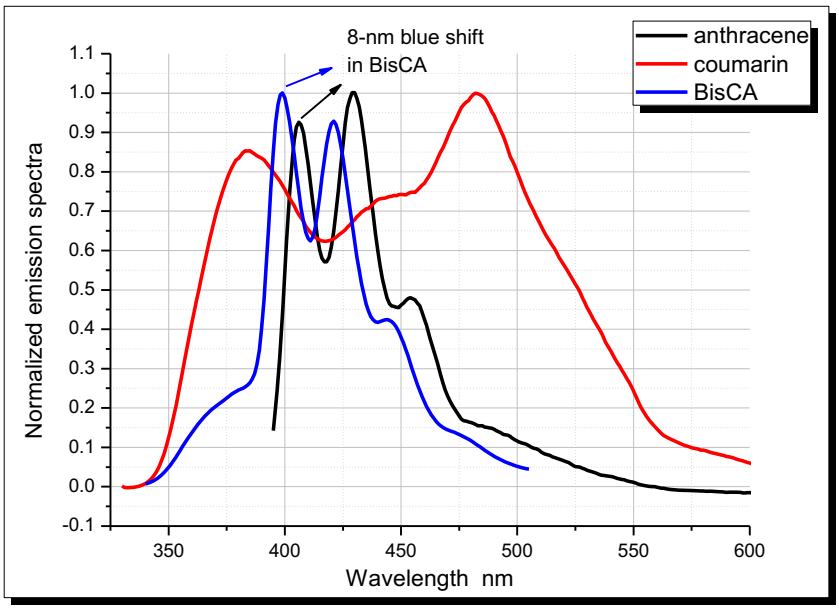

Fig. 5 Normalized emission spectra of 1×10^{-5} M three dyes in ethanol

Table 1 Optical and photo—physical properties of three dyes in different solvents

	$\varepsilon \times 10^3$ (L M^{-1} Cm^{-1})	Stocks shift cm^{-1}	Φf	$\sigma_a x10^{-16}$ (Cm^2)	$\sigma_e x10^{-23}$ (Cm^2)	T (ns)	*F*	μ (D)	E_f	Λ (cm)	$K_{nrd} \times 10^9$ (s^{-1})	$K_{rad} \times 10^9$ (S^{-1})
Coum./DMF	27	4930	0.15	1.02	1.87	0.18	0.18	12.7	0.13	1.6	4.6	5.5
Coum./EtOHl	25	9253	0.21	0.96	5.65	0.1	0.21	15.4	0.14	1.7	7.9	10
Coum. /Toulene	20	6084	0.054	0.77	1.96	0.05	0.19	13.4	0.04	2.1	18	20
Anth../DMF	16.6	2357	0.31	0.63	33	0.04	0.18	13.3	0.28	2.61	17	25
Anth./Ethanol	16.2	2990	0.15	0.61	10	0.07	0.58	24.2	0.13	2.68	12	14
Anth./Toulene	17	2854	0.06	0.65	5.2	0.05	0.21	14.5	0.05	2.5	18	20
BisCA/DMF	27	7854	0.35	1.03	1.63	0.66	0.18	13.5	0.26	1.6	0.98	1.5
BisCA/Ethanol	40	6187	0.42	1.52	19	0.07	0.12	10.6	0.33	1.08	8.2	14
BisCA/Toulene	33	7797	0.34	1.25	3.4	0.34	0.17	13.1	0.25	1.3	1.9	2.9
BisCA/Acetic acid	35	5739	0.48	1.33	2.75	0.38	0.22	14.3	0.39	1.2	1.3	2.6
BisCA/Xylene	32	8227	0.3	1.2	1.6	0.06	0.17	13.0	0.22	1.35	10	16
BisCA/Acetone	19	6356	0.27	0.72	1.48	0.47	0.12	10.6	0.21	2.28	1.5	2.1

A Debye (D) is the traditional non-SI unit of dipole moment. The conversion between D and SI units is 1Dp = 2.36 × 10^{-30} (coulomb. meter).

Since an excited dye molecule can return to the ground state by a number of pathways, either intramolecular or intermolecular interactions, [44] the fluorescence quantum yield is directly related to the radiative (k_r) and nonradiative (k_{nr}) rate constants of deactivation by the relationship (15) [44].

$$\phi_f = \frac{k_r}{k_r + k_{nr}} \tag{15}$$

This parameter has major importance not only since it is a physical characteristic of a molecule in specific conditions but it is also ultimately involved in the calculation of quenching-rate constants, energy transfer, lasing ability and radiative or nonradiative rate constants, from which the whole photophysical behavior can be deduced.

However, the radiative (fluorescence) decay rate constant (k_r) of a probe can be assessed from Eq. (16) based on Strickler-Berg equation, which depends on Einstein's spontaneous emission rate and Planck's black body radiation law [45].

$$k_r = \frac{1}{\tau_0} = 2.88 \times 10^{-9} n^2 \frac{\int F\left(\tilde{\nu}\right) d\nu}{\int F\left(\tilde{\nu}\right) \tilde{\nu}^{-3} d\nu} \int \frac{\varepsilon\left(\tilde{\nu}\right)}{\tilde{\nu}} d\tilde{\nu}, \tag{16}$$

Where $F(\tilde{\nu})$, $\tilde{\nu}$, $\varepsilon(\tilde{\nu})$ are the fluorescence intensity, wavenumber and molar extinction coefficient at a certain wavenumber ($\tilde{\nu}$), respectively, while *n* is the refractive index of the medium.

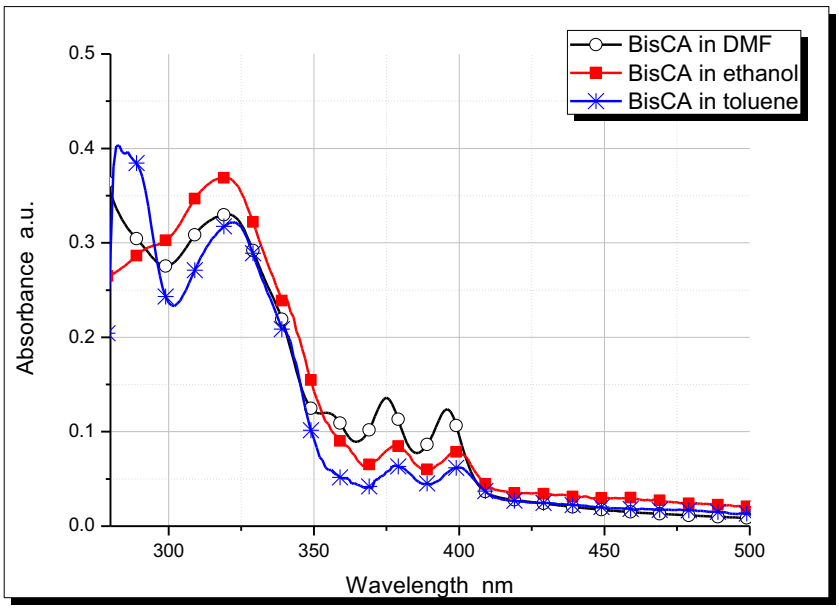

Fig. 6 Absorption of BisCA in different solvents

Results and Discussion

Synthesis and Characterization of BisCA

The synthetic utility of 7-hydroxy-4-methylcoumarin (**1**) as building block for novel bis(coumarin) **3** was investigated as outlined in Scheme 1. Thus, the reaction of the potassium salt (obtained upon treatment of **1** with ethanolic KOH), with 9,10-bis(bromomethyl)anthracene (**2**) in boiling DMF afforded 7,7′-((anthracene-9,10-diylbis(methylene))bis(oxy))bis(4-methyl-2*H*-chromen-2-one) (**3**) (BisCA) in 81% yield.

Compound **3** (BisCA) was characterized by elemental analyses, as well as its spectral data which agree with the proposed structure. Thus, the IR spectrum of **3** exhibits an absorption band at υ 1714 cm^{-1} characteristic for the carbonyl group. Moreover, the absence of an absorption band corresponding to OH stretching frequency of the parent coumarin **1** in the IR spectrum of the alkylated product clearly confirmed the formation of BisCA **3**. Moreover, the ^{1}H NMR spectra in Fig. 1 of BisCA showed a singlet signal at δ 2.39 integrated for six protons attributed to the methyl protons together with a singlet signal at δ 5.42 integrated for four protons characteristic for the OCH_2 protons. In addition, ^{1}H NMR spectra displays a singlet signal at δ 6.19 integrated for two protons attributed to the coumarin protons. All other protons were seen at the expected chemical shifts and integral values. Mass analysis of compound **3** showed an intense molecular ion peak at m/z 554, in agreement with their respective molecular formulae.

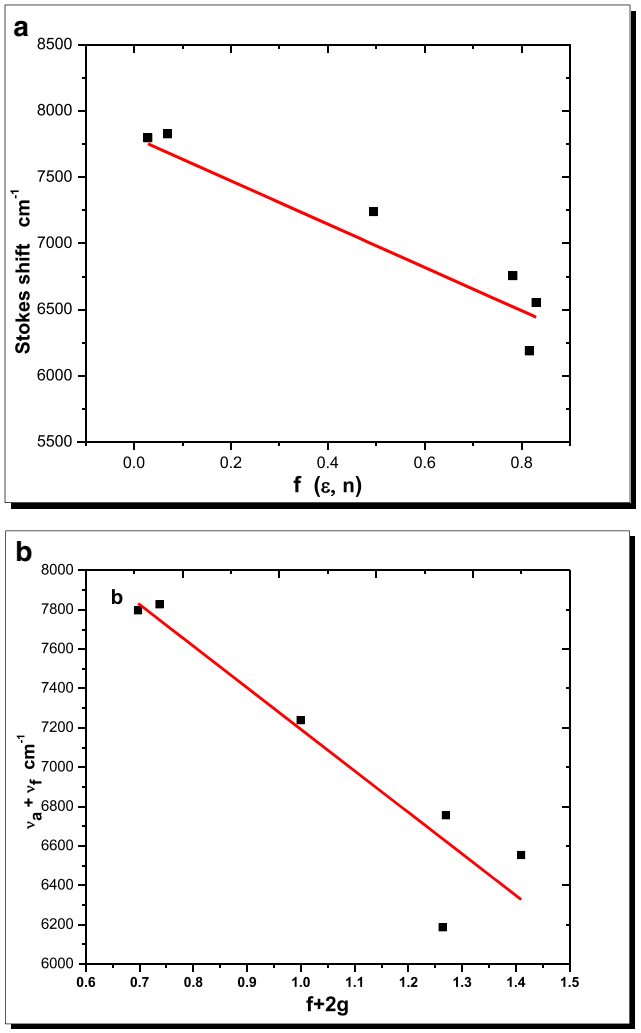

Fig. 8 Stockes shifts of BisCA dye versus different solvent polarity function (**a**) f(ε,n) and (**b**) f(ε,n) + 2 g(n)

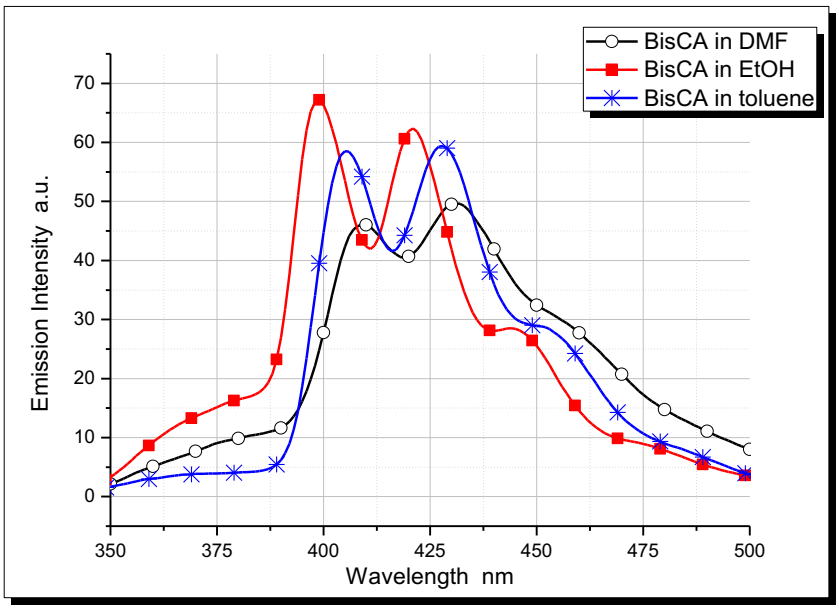

Fig. 7 Emission of BisCA in different solvents

Optical Properties of Bis(coumarinyl) Anthracene (BisCA)

As shown in Fig. 2 which represents the absorption spectra of three dyes in DMF as aprotic solvent. The absorption spectra of BisCA is presented by broad band ranged from 280 nm to 415 nm of two separated characterized profiles. BisCA absorption spectra has a combination profile spectra of coumarin dye, which is broad band spectrum at maximum wavelength 320 nm, and anthracene dye which characterized by three fine spectral peaks at 355, 374 and 396 nm. The large bulk structure of BisCA molecule and intramolecular charge transfer (ICT) in coumarin part may result in decreasing of ground state energy of anthracene in BisCA compared with parent 9,10-dibromro anthracene probe (10 nm blue shift was noticed). There is no shifting in coumarin part of BisCA compared with parent coumarin, which may be attributed to the charge transfer resonance in coumarin part with lone-pair of etheric oxygen atom as shown in Scheme 2.

The effect of protic solvent such as ethanol on electronic absorption spectra of BisCA is presented in Fig. 3. This spectra show about 5 nm red-shift of absorption spectra of BisCA compared with the corresponding one in aprotic solvent (DMF) in both coumarin and anthracene parts. The shifting may be attributed to intermolecular hydrogen bond donar (HBD) character of ethanol. The maximum peak of absorption spectrum of coumarin dye exhibits a higher wavelength absorption compared with its respective peak in BisCA probe due to dual inter-and intramolecular H-bond interactions of coumarin dye with itself as well as with protic environment. On the other hand, only intermolecular H-bond interaction occur in BisCA molecule.

Table 2 Dipole moments, slope (m) of BisCA dye by Bakhshiev and Reichardt methods

Method	$m_1(cm^{-1})$	$m_2(cm^{-1})$	μ_e-μ_g	μ_g(D)	μ_e(D)
Bakhshiev	634.6	1663.8	6. 87	75.78	82.65
Reichardt			13.9		

Normalized emission spectra of three dyes in aprotic solvent (i.e. DMF as shown in Fig. 4 shows a red-shift in fine band peaks of anthracene part of BisCA probe compared with its precursor anthracene dye. This shifting in fluorescence spectra indicates the higher stability of excited state of BisCA in aprotic solvent. This lower electronic energy of excited state of BisCA compared with that of the parent anthracene probe (9,10-dibromomethylanthracene) may be attributed to lower electronegativity of bromine atom compared with electron-withdrawing effect of etheric oxygen atom in BisCA dye.

On the other hand, protic solvent effect in Fig. 5 shows different fluorescence behavior of all dyes. Firstly, coumarin dye shows extra two new peaks in longer wavelengths (at 442 & 483 nm) which attributed to intermolecular H-bond interaction with solvent molecules. Anthracene part in BisCA dye has 8-nm blue shift compared with that of parent anthracene dye. This may be attributed to the increase of the excited state energy as a result of increasing the steric geometry of BisCA molecule by H-bond formation of its coumarin moiety with the protic ethanol solvent. The effect of prtoic and aprotic solvents on the spectral data, Stokes shift, photo physical parameters of three dyes were assessed under the same conditions and tabulated in Table 1.

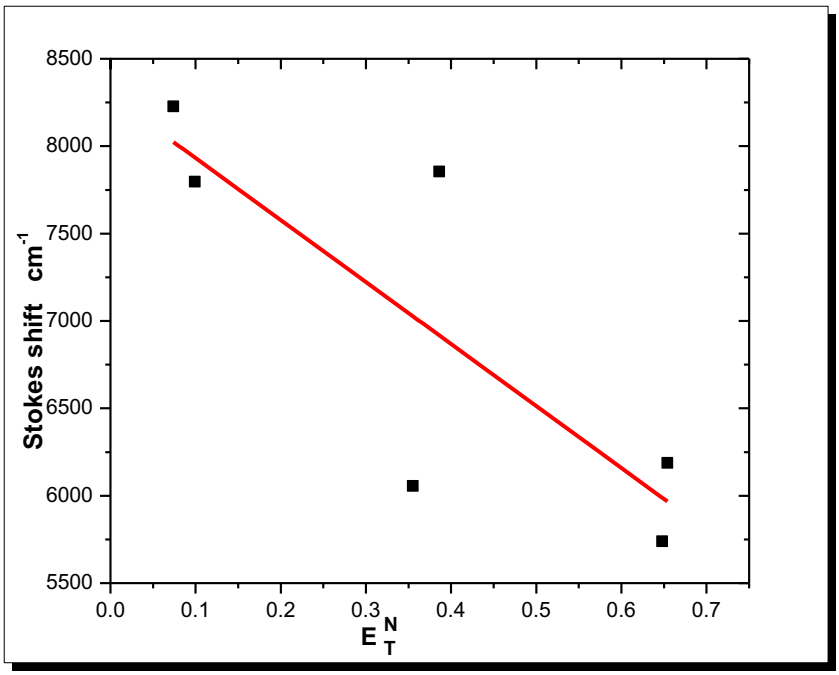

Fig. 9 Stockes shifts of BisCA dye versus the microscopic solvent polarity of different solvents (E_T^N)

Solvent Polarity and H-Bonding Effect on Bis(coumarinyl) Anthracene BisCA

Solvent polarity simply defined as the overall solvation capability of solvents, which in turn depends on the action of all possible, nonspecific and specific, intermolecular interactions between solute molecules and solvent molecules, excluding, however, those interactions leading to definite chemical alterations of the solute molecules (such as oxidation, reduction, protonation, chemical complex formation etc.) [46, 47].

As shown in Fig. 6, the absorption spectra of BisCA probe has different trend in its two chromophore parts. However, the highest absorption intensity of the coumarin chromophore part was recorded in ethanol, while in anthracene chromophore part, the highest absorption intensity was recorded in DMF with slight blue shift. This different behavior may be attributed to the higher polarity of coumarin compared with anthracene.

As we noticed in Fig. 7, the emission spectra of BisCA probe which excited by wavelength of 323 nm in different solvents has the highest intensity in protic solvent (ethanol). This may be explained in terms of the intramolecular hydrogen bond with ethanol. On the other hand, blue shift in anthracene part may referred to intra charge transfer (ICT) in both coumarin sides of BisCA through etheric oxygen atom leading to increase of the electronic energy of excited state in anthracene part. In toluene, the slight red- shift in the maximum wavelength position (at 410 nm and 430 nm) may attributed to its low solvent polarity. However, decreasing in intersystem crossing efficiency is due to an increase in the energy of $n \rightarrow \pi^*$ triplet state resulting in an increase of radiative fluorescence efficiency. In DMF a decrease of fluorescence efficiency with small red shift of the anthracene part of BisCA was assessed.

The effect of solvent polarity by either microscopic or functionally methods using six solvents (ethanol & acetic acid as protic polar, DMF & acetone as aprotic polar and toluene & xylene as non-polar solvents) was also investigated. Thus, the solvents effect on Stokes shifts was shown in Figs. 8a, b and 9. Also, their effects on some photo-physical parameters of probe were assessed and compiled in Tables 1 and 2. It is noticed that, Stokes shifts have the lowest values in case of protic polar solvents, while it has the highest value in non-polar solvents.

On the other hand, BisCA dye has the highest fluorescence quantum yields (i.e. $\varphi_f = 0.42$ and 0.48 in ethanol and acetic acid, respectively) in protic polar solvents. While the lowest fluorescence quantum yield (i.e. $\varphi_f = 0.27$ in acetone) was observed in non-polar solvent.

Finally, according to Bakhshiev and Reichardt equations [30, 31, 36] the dipole moment of BisCA was assessed and tabulated in Table 2.

Conclusion

Molar absorptivity, oscillator strength, transition dipole moment, excited-state lifetime, fluorescence quantum yield, absorption as well as emission cross sections, rate of radiative and non-radiative decay for our new target probe BisCA and its fluorescent starting materials have been deduced in various organic solvents. The characterized Onsager cavity radiuses as well as the dipole moments of ground and excited state according to Bakhshiev and Reichardt methods were estimated.

Intermolecular H-bonding interaction between dye molecules and solvent molecules was found to have distinctive impact on optical and photophysical properties of the focused probe. This may occur as a result of different factors related to geometrical chemical structure of probe, strengthening H-bond formation and physical properties of surrounding media.

References

1. Reineke S, Lindner F, Schwartz G, Seidler N, Walzer K, Lussem B, Leo K (2009) White organic light-emitting diodes with fluorescent tube efficiency. Nature 459:234–238
2. Suarez MF, Ting AY (2008) Fluorescent probes for super-resolution imaging in living cells. Nat Rev Mol Cell Biol 9:929–943
3. Cursino ACT, Gardolinski J, Wypych F (2010) Intercalation of anionic organic ultraviolet ray absorbers into layered zinc hydroxide nitrate. J Colloid Interface Sci 347:49–55
4. Zeng WD, Cao YM, Bai Y, Wang YH, Shi YS, Zhang M, Wang FF, Pan CY, Wang P (2010) Efficient dye-sensitized solar cells with an organic photosensitizer featuring orderly conjugated Ethylenedioxythiophene and Dithienosilole blocks. Chem Mater 22:1915–1925
5. Xiao LX, Chen ZJ, Qu B, Luo JX, Kong S, Gong QH, Kido JJ (2011) Recent progresses on materials for electrophosphorescent organic light-emitting devices. Adv Mater 23:926–952
6. Hu ZC, Deibert BJ, Li J (2014) Luminescent metal–organic frameworks for chemical sensing and explosive detection. Chem Soc Rev 43:5815–5840
7. Kumari N, Jha S, Bhattacharya S (2011) Colorimetric probes based on Anthraimidazolediones for selective sensing of fluoride and cyanide ion via intramolecular charge transfer. J Organomet Chem 76: 8215–8222
8. Zhou JM, Shi W, Xu N, Cheng P (2013) Highly selective luminescent sensing of fluoride and organic small-molecule pollutants based on novel lanthanide metal–organic frameworks. Inorg Chem 52:8082–8090
9. Capobianco ML, Barbarella G, Manetto A (2012) Oligothiophenes as fluorescent markers for biological applications. Molecules 17: 910–933
10. Chen SJ, Liu JZ, Liu Y, Su HM, Hong YN, Jim CKW, Kwok RTK, Zhao N, Qin W, Lam JWY, Wong KS, Tang BZ (2012) An AIE-active hemicyanine fluorogen with stimuli-responsive red/blue emission: extending the pH sensing range by "switch + knob" effect. Chem Sci 3:1804–1809
11. Benniston AC, Harriman A, Yang SJ (2013) Providing power for miniaturized medical implants: triplet sensitization of semiconductor surfaces. Philos Trans Roy Soc A Math Phys Eng Sci 371: 20120334

12. Fang H, Xu B, Li X, Kuhn DL, Zachary Z, Chen GTV, Chu R, DeLacy BG, Rao Y, Dai H-L (2017) Effects of molecular structure and solvent polarity on adsorption of carboxylic anchoring dyes onto TiO_2 particles in aprotic solvents. Langmuir 33:7036–7042
13. Tan A, Bozkurt E, Kara Y (2017) Investigation of solvent effects on Photophysical properties of new Aminophthalimide derivatives-based on Methanesulfonate. J Fluoresc 27:981–992
14. Lu G, Jiang X, Oua Z, Yana S, Kadish KM (2017) Solvent and substituent effects on UV-Vis spectra and redox properties of zinc p-hydroxylphenylporphyrins. J Porphyrins Phthalocyanines 21:1–11
15. Woodford O, Harriman A, McFarlane W, Wills C (2017) Dramatic effect of solvent on the rate of photo-bleaching of organic (BOPHY) dyes. Chemphotochem 1:317–325
16. Kim JY, Hwang TG, Woo SW, Lee JM, Namgoong JW, Yuk SB, Chung S-w, Kim JP (2017) Simple modification of basic dyes with bulky & symmetric WCAs for improving their solubilities in organic solvents without color change. Sci Rep 7:46178
17. Hu X, Liu Y, Duan Y, Han J, Li Z, Han T (2017) A turn-on type stimuli-responsive fluorescent dye with specific solvent effect: implication for a new prototype of paper using water as the ink. Spectrochim Acta A 184:7–12
18. Zhao GJ, Han KL (2007) Ultrafast hydrogen bond strengthening of the Photoexcited Fluorenone in alcohols for facilitating the fluorescence quenching. J Phys Chem A 111:9218–9223
19. Zhou L-C, Liu J-Y, Zhao G-J, Shi Y, Peng X-J, Han K-L (2007) The ultrafast dynamics of near-infrared heptamethine cyanine dye in alcoholic and aprotic solvents. Chem Phys 333:179–185
20. Li G-Y, Zhao G-J, Han K-L, He GZ (2011) A TD-DFT study on the cyanide-chemosensing mechanism of 8-formyl-7-hydroxycoumarin. J Comput Chem 32:668–674
21. Pal SK, Mandal D, Bhattacharyya K (1998) Photo-physical processes of ethidium bromide in micelles and reverse micelles. J Phys Chem B 102:11017–11023
22. Jimenez R, Fleming GR, Kumar PV, Maroncelli M (1994) Femtosecond solvation dynamics of water. Nature 369:471–473
23. Heilweil EJ (1999) Ultrafast glimpses at water and ice. Science 283: 1467–1468
24. Liu Y-H, Zhao G-J, Li G-Y, Han KL (2010) Fluorescence quenching phenomena facilitated by excited-state hydrogen bond strengthening for fluorenone derivatives in alcohols. J Photochem Photobiol A Chem 209:181–185
25. Chai S, Zhao G-J, Song P, Yang S-Q, Liu J-Y, Han K-L (2009) Reconsideration of the excited-state double proton transfer (ESDPT) in 2-aminopyridine/acid systems: role of the intermolecular hydrogen bonding in excited states. Phys Chem Chem Phys 11: 4385–4390
26. Zhao G-J, Han K-L (2008) Effects of hydrogen bonding on tuning photochemistry: concerted hydrogen-bond strengthening and weakening. Chem Phys Chem 9:1842–1846
27. Fahmy HM, Negm NA, Elwahy AHM, Abou Kana MTH (2017) Laser induced fluorescence, photo-physical parameters and photostability of new fluorescein derivatives. J Mol Liq 229:31–44
28. El Wahy AHM, Ismail AR, Abou Kana MTH, Negm NA (2017) Synthesis and characterization of novel bis-(4-methylcoumarin) derivatives as photosensitizers in antimicrobial photodynamic therapy. J Taiwan Inst Chem Eng 77:83–91
29. Negm NA, Abou Kana MTH, Abd-Elaal AA, Elwahy AHM (2016) Fluorescein dye derivatives and their nanohybrids: synthesis, characterization and antimicrobial activity. J Photochem Photobio B: Biology 162:421–433
30. Bakhshiev NG (1962) Universal intermolecular interactions and their effect on the position of the electronic spectra of molecules in two component solutions. Opt Spectrosk 13:24–29
31. Bakhshiev NG (1972) Spektroskopija mezhmolekuljarnyh vzaimodestvii Izd. Nauka, Leningrad
32. Tipperudrappa J, Biradar DS, Manohara SR, Hanagodimath SM, Inamdar SR, Mannekutla JR (2008) Solvent effects on the absorption and fluorescence spectra of some laser dyes: estimation of ground and excited-state dipole moments. J Spectrochim Acta, Part A 69:991–997
33. Ooshika Y (1954) Absorption spectra of dyes in solution. J Phys Soc Jpn 9:594–602
34. Suppan P (1983) Excited-state dipole moments from absorption / fluorescence solvatochromic ratios. Chem Phys Lett 94:272–275
35. Homocianu M, Airinei A, Dorohoi DO (2011) Solvent effects on the electronic absorption and fluorescence spectra. J Adv Res Phys 2:011105
36. Reichardt C (2004) Solvents and solvent effect in organic chemistry, 3rd edn. Wiley-VCH, Verlag, GmbH and Co., KGaA, Weinheim
37. Ravi M, Soujanya T, Samanta A, Radhakrishnan TR (1995) Excited-state dipole moments of some Coumarin dyes from a solvatochromic method using the solvent polarity parameter, E_T^N. J Chem Soc Faraday Trans 91:2739
38. Ruland G, Gvishi R, Prasad PN (1996) Multiphasic nanostructured composites: multidye tunable solid-state laser. J Am Chem Soc 118: 2985–2991
39. Deshpande AV, Namdas EB (1996) Efficient lasing action of rhodamine 6G in Nafion membranes. J Chem Phys Letter 263:449–455
40. Kumar S, Rao VC, Rastogi RC (2001) Excited-state dipole moments of some hydroxycoumarin dyes using an efficient solvatochromic method based on the solvent polarity parameter E_T^N. J Spectrochimica Acta Part A 57:41–47
41. Patel DR, Patel NB, Patel BM, Patel KC (2014) Synthesis and dyeing properties of some new monoazo disperse dyes derived from 2-amino-4-(2,4-dichlorophenyl)-1,3-thiazole. J Saudi Chem Soc 18:902–913
42. Saeed A, Shabir G (2014) New fluorescent symmetrically substituted perylene-3,4,9,10-dianhydride-azohybrid dyes: synthesis and spectroscopic studies. Spectrochimica Acta A: Molecular and Biomolecular Spec 133:7–12
43. Bojinov V, Grabchev I (2004) Synthesis and photophysical investigations of novel combined benzo[*de*]anthracen-7-one/2,2,6,6-tetramethyl piperidines as fluorescent stabilisers for polymer materials. J Polymer Degradation and Stability 85:789–797
44. Forgues SF, Lavabre D (1999) Are fluorescence quantum yields so tricky to measure? A demonstration using familiar stationery products. J Chem Educ 76:1260
45. Kumar GA, Unnikrishnan NV (2001) Energy transfer and optical gain studies of FDS: Rh B dye mixture investigated under cw laser excitation. J Photochem Photobio A 144:107–114
46. Reichardt C (1988) Solvents and solvent effects in organic chemistry, 2nd edn. VCH Publishers, Weinheim
47. Streitwieser A, Heathcock CH, Kosower EM (1992) Introduction to organic chemistry, 5th edn. McMillan, New York, pp 677–678